INFECTION AND IMMUNITY, Nov. 2002, p. 6373–6382 Vol. 70, No. 11
0019-9567/02/$04.00+0 DOI: 10.1128/IAI.70.11.6373–6382.2002

Staphylococcus aureus Aconitase Inactivation Unexpectedly Inhibits Post-Exponential-Phase Growth and Enhances Stationary-Phase Survival

Greg A. Somerville,[1] Michael S. Chaussee,[1]† Carrie I. Morgan,[1]‡ J. Ross Fitzgerald,[1] David W. Dorward,[2] Lawrence J. Reitzer,[3] and James M. Musser[1]*

Laboratory of Human Bacterial Pathogenesis[1] and Rocky Mountain Microscopy Branch,[2] Rocky Mountain Laboratories, National Institute of Allergy and Infectious Diseases, National Institutes of Health, Hamilton, Montana 59840, and Department of Molecular and Cellular Biology, The University of Texas at Dallas, Richardson, Texas 75083[3]

Received 13 June 2002/Returned for modification 12 July 2002/Accepted 24 July 2002

Staphylococcus aureus **preferentially catabolizes glucose, generating pyruvate, which is subsequently oxidized to acetate under aerobic growth conditions. Catabolite repression of the tricarboxylic acid (TCA) cycle results in the accumulation of acetate. TCA cycle derepression coincides with exit from the exponential growth phase, the onset of acetate catabolism, and the maximal expression of secreted virulence factors. These data suggest that carbon and energy for post-exponential-phase growth and virulence factor production are derived from the catabolism of acetate mediated by the TCA cycle. To test this hypothesis, the aconitase gene was genetically inactivated in a human isolate of *S. aureus*, and the effects on physiology, morphology, virulence factor production, virulence for mice, and stationary-phase survival were examined. TCA cycle inactivation prevented the post-exponential growth phase catabolism of acetate, resulting in premature entry into the stationary phase. This phenotype was accompanied by a significant reduction in the production of several virulence factors and alteration in host-pathogen interaction. Unexpectedly, aconitase inactivation enhanced stationary-phase survival relative to the wild-type strain. Aconitase is an iron-sulfur cluster-containing enzyme that is highly susceptible to oxidative inactivation. We speculate that reversible loss of the iron-sulfur cluster in wild-type organisms is a survival strategy used to circumvent oxidative stress induced during host-pathogen interactions. Taken together, these data demonstrate the importance of the TCA cycle in the life cycle of this medically important pathogen.**

Staphylococcus aureus is a gram-positive pathogen that causes a wide variety of diseases in humans and animals, ranging from local soft-tissue infections to life-threatening septicemia. *S. aureus* causes disease by producing many extracellular virulence factors, including several proteases, lipases, hemolysins, superantigens, and cell wall-associated adherence proteins. As with many pathogens, maximal expression of *S. aureus* virulence factors occurs during the post-exponential phase of growth (33). Bacteria exit from the exponential phase of growth upon the depletion of readily catabolizable carbon compounds and/or the accumulation of toxic compounds. During growth in vitro, *S. aureus* preferentially degrades glucose to pyruvate (9, 18, 22, 28) by way of the pentose phosphate and glycolytic pathways (4). The catabolic fate of pyruvate is determined by the growth conditions. Under anaerobic growth conditions, pyruvate is primarily reduced to lactic acid (22, 24), while it is oxidized to acetate and CO_2 under aerobic growth conditions (16). The ability to oxidize acetate in the exponential phase of growth is severely impaired, and acetate accumulates in the culture medium until the glucose has been depleted (9, 18). Thus, maximal expression of virulence factors coincides with the depletion of glucose, entry into the post-exponential phase of growth, and the catabolism of acetate. Taken together, these data suggest that the carbon and energy needed for post-exponential-phase growth and virulence factor production are primarily derived from the catabolism of acetate.

Acetate in the form of acetyl-coenzyme A (CoA) can be oxidized by the tricarboxylic acid (TCA) cycle when *S. aureus* is grown in the presence of certain TCA cycle intermediates (18). Therefore, it is reasonable to hypothesize that inactivation of the TCA cycle would detrimentally affect acetate catabolism, growth, and virulence factor production. To test this hypothesis, aconitase (EC 4.2.1.3) was genetically inactivated in a low-passage human isolate of *S. aureus*, and growth, glucose-acetate catabolism, virulence factor production, and virulence for mice were characterized.

* Corresponding author. Mailing address: Laboratory of Human Bacterial Pathogenesis, Rocky Mountain Laboratories, National Institute of Allergy and Infectious Diseases, National Institutes of Health, 903 South 4th St., Hamilton, MT 59840. Phone: (406) 363-9315. Fax: (406) 363-9427. E-mail: jmusser@niaid.nih.gov.

† Present address: Division of Basic Biomedical Sciences, University of South Dakota College of Medicine, Vermillion, SD 57069-2390.

‡ Present address: University of Kentucky College of Medicine, Lexington, KY 40536.

MATERIALS AND METHODS

Bacterial strains, plasmids, and materials. The strains and plasmids used in this study are listed in Table 1. *Escherichia coli* strains were grown in 2× YT broth or on 2× YT agar (34). *S. aureus* strains were grown in tryptic soy broth containing 0.25% glucose (TSB) (BD Biosciences, Sparks, Md.) or on TSB containing 1.5% agar. All antibiotics were purchased from Sigma Chemical Co. (St. Louis, Mo.) and were used at the following concentrations: ampicillin, 100 μg/ml (*E. coli*); erythromycin, 8 μg/ml, and chloramphenicol, 7.5 μg/ml (*S. aureus*).

TABLE 1. Strains and plasmids used in this study

Plasmid or strain	Relevant genotype or characteristic(s)	Source or reference
pBluescript II KS(+)	*E. coli* phagemid cloning vector	Stratagene
pTS1	*S. aureus-E. coli* temperature-sensitive shuttle vector	19
pEC4	pBluescript II KS(+) with *ermB* inserted into *Cla*I site	5
pGAS-4	pBluescript II KS(+) containing an internal fragment of the *acnA* gene of RN6390 inserted into *Sma*I site	This study
pGAS-5	pGAS-4 containing the *ermB* cassette of pEC4 inserted into the *Nsi*I site of the *acnA* fragment	This study
pGAS-6	The *acnA*::*ermB* PCR product from pGAS-5 inserted into the *Sma*I site of pTS1	This study
RN4220	Restriction-negative *S. aureus*	32
SA564	Recent human *S. aureus* isolate	J. M. Musser
SA564-*acnA*::*ermB*	SA564 containing an *ermB* insertion into *acnA*	This study

***S. aureus* aconitase mutant construction.** A 1-kb internal fragment (nucleotides 1191 to 2195 relative to the start codon) was amplified by PCR and cloned into the *Sma*I site of pBluescript II K/S(+) (Stratagene) to generate the plasmid pGAS-4. The *ermB* cassette of pEC4 (5) was inserted into the *Nsi*I site contained within the *acnA* fragment of pGAS-4 to yield the plasmid pGAS-5. The *acnA*::*ermB* fragment was PCR amplified and cloned into the *Sma*I site of the temperature-sensitive plasmid pTS1 (19) to generate the plasmid GAS-6. The temperature-sensitive plasmid pGAS-6 was isolated from *S. aureus* strain RN4220 (32) and was introduced into strain SA564 by electroporation (35). The transformed strain was then used to construct an aconitase mutant by the method described by Foster (15). Putative mutants were analyzed by PCR and Southern blotting (38) and assayed for aconitase activity.

Enzymatic-activity assays. Cell lysates of *S. aureus* were prepared as follows. Aliquots (3 ml) were harvested at the appropriate times and resuspended in 1.5 ml of lysis buffer containing 90 mM Tris (pH 8.0), 100 μM fluorocitrate, and 50 μg of lysostaphin (Sigma)/ml. The samples were incubated at 37°C for 10 min and passed through a French press (two times at 15,000 lb/in^2). The lysate was centrifuged for 5 min at 20,800 × *g* and 4°C. Aconitase activity was assayed in the resulting cell lysate by the method described by Kennedy et al. (23). One unit of aconitase activity is defined as the amount of enzyme necessary to give a ΔA_{240} min^{-1} of 0.0033 (3). Protein concentrations were determined by the method of Lowry et al. (26).

Measurement of citrate, acetate, glucose, lactate, and ammonia in culture supernatants. Aliquots of bacteria (1.5 ml) were centrifuged for 5 min at 20,800 × *g* in a refrigerated centrifuge. The culture supernatants were adjusted to pH 8 with KOH. Citrate, acetate, glucose, lactate, and ammonia concentrations were determined with kits purchased from R-Biopharm, Inc. (Marshall, Mich.) and used according to the manufacturer's directions.

Determination of stationary-phase survival. Single colonies of SA564 and SA564-*acnA*::*ermB* were inoculated into 1-liter flasks containing 100 ml of TSB, grown at 37°C, and aerated by shaking them at 225 rpm for up to 2 weeks. Aliquots (200 μl) were taken at 24-h intervals, and the CFU per milliliter were determined on TSB containing 1.5% agar. Sterile deionized water was added as needed to offset the evaporative loss of water.

Two-dimensional electrophoresis and protein identification. Procedures for two-dimensional electrophoresis and identification of proteins by matrix-assisted laser desorption ionization–time of flight mass spectrometry (MALDI-TOF MS) have been described previously (6). Equivalent quantities of total protein (80 μg) were used in each two-dimensional (2-D) electrophoresis experiment.

Determination of virulence factor production. Hemolytic activity, staphylokinase activity, and the presence of clumping factor were determined as described previously (14). Lipase activity was measured with the Lipase-PS kit (Sigma). The relative quantity of staphylococcal enterotoxin C (SEC) was determined by enzyme-linked immunosorbent assay with a monoclonal antibody to SEC (IGEN International, Inc., Gaithersburg, Md.). The quantity of SEC is expressed as the amount of horseradish peroxidase-induced absorbance at 405 nm per picogram of total protein (A_{405} per picogram). The total protease activity present in culture supernatants was determined by use of the Universal Protease Substrate (Roche Molecular Biochemicals, Indianapolis, Ind.).

Electron microscopy. Samples of staphylococci were prepared for scanning electron microscopy as described previously (13). The prepared samples were examined with a Hitachi S4500 field emission scanning electron microscope. The maximum bacterial cell lengths were determined from multiple measurements ($n \geq 40$) of bacterial samples prepared from single cultures of SA564 and SA564-*acnA*::*ermB*. Bacterial cell measurements and statistical analyses were performed using SigmaScan Pro version 5.0 software (SPSS Science, Chicago, Ill.).

Staphylococci were prepared for transmission electron microscopy essentially as described previously (29).

Northern blot analysis. Northern blot analyses of RNAIII, *sarA*, and *sigB* transcripts were performed as described previously (34). The blot was probed with [^{32}P]dATP-labeled (RadPrime DNA-labeling kit; Gibco BRL) PCR products amplified from SA564 genomic DNA. The integrated density values of bands on autoradiographs were determined with AlphaImager 2000 software (Alpha Innotech Corp., San Leandro, Calif.).

Mouse virulence. The virulences of the *S. aureus* aconitase mutant and isogenic wild-type strains were assessed with a mouse soft-tissue infection model (27). The bacteria were incubated for 3 h, harvested, washed once with ice-cold phosphate-buffered saline, frozen in liquid nitrogen, and stored at −80°C. The CFU per milliliter were determined before the bacteria were frozen and confirmed when the mice were inoculated. For the soft-tissue infection model, 25 outbred, immunocompetent, hairless mice (Crl::SKH1-hrBR) were inoculated subcutaneously. The mice were weighed prior to inoculation and once a day after inoculation until they regained their preinoculation weight. The statistical significances of the percentage of body weight lost and the average number of days to regain the lost body weight were assessed with Student's *t* test.

All experiments involving animals were reviewed and approved by the Rocky Mountain Laboratories Animal Care and Use Committee and complied with animal welfare legislation and National Institutes of Health guidelines and policies.

RESULTS

***S. aureus* aconitase mutant growth.** Insertional inactivation of the single aconitase (*acnA*) gene in *S. aureus* strain SA564 by allelic replacement was verified by PCR and Southern blot analysis (Fig. 1A). Additionally, inactivation was confirmed by assaying aconitase activity. No detectable aconitase activity (<0.1 U mg of protein^{-1}) was found in the mutant, whereas the isogenic strain had 141.0 U mg of total protein^{-1}, confirming the presence of a single aconitase in *S. aureus* (Fig. 1B). The doubling time, the length of the exponential growth phase, and the exponential-phase acidification of the culture medium of the *acnA* mutant (SA564-*acnA*::*ermB*) were equivalent to those of the isogenic wild-type strain (Fig. 1C). These data suggest that TCA cycle activity is not growth limiting in wild-type *S. aureus* during the exponential growth phase, consistent with previous observations that have demonstrated TCA cycle repression (18, 40). Unexpectedly, TCA cycle inactivation caused *S. aureus* to enter the stationary phase of growth prematurely (Fig. 1C). This surprising result occurred in a rich medium containing glucose and free amino acids, suggesting an inability to catabolize available carbon sources.

We expected that the premature entry of the aconitase mutant into the stationary phase of growth would result in early entry into the death phase. To test this hypothesis, we assessed the stationary-phase survival of SA564-*acnA*::*ermB* and SA564. Single colonies were inoculated into TSB and grown aerobically for up to 2 weeks, and the CFU per milliliter were determined daily. An aconitase mutant in the phylogenetically

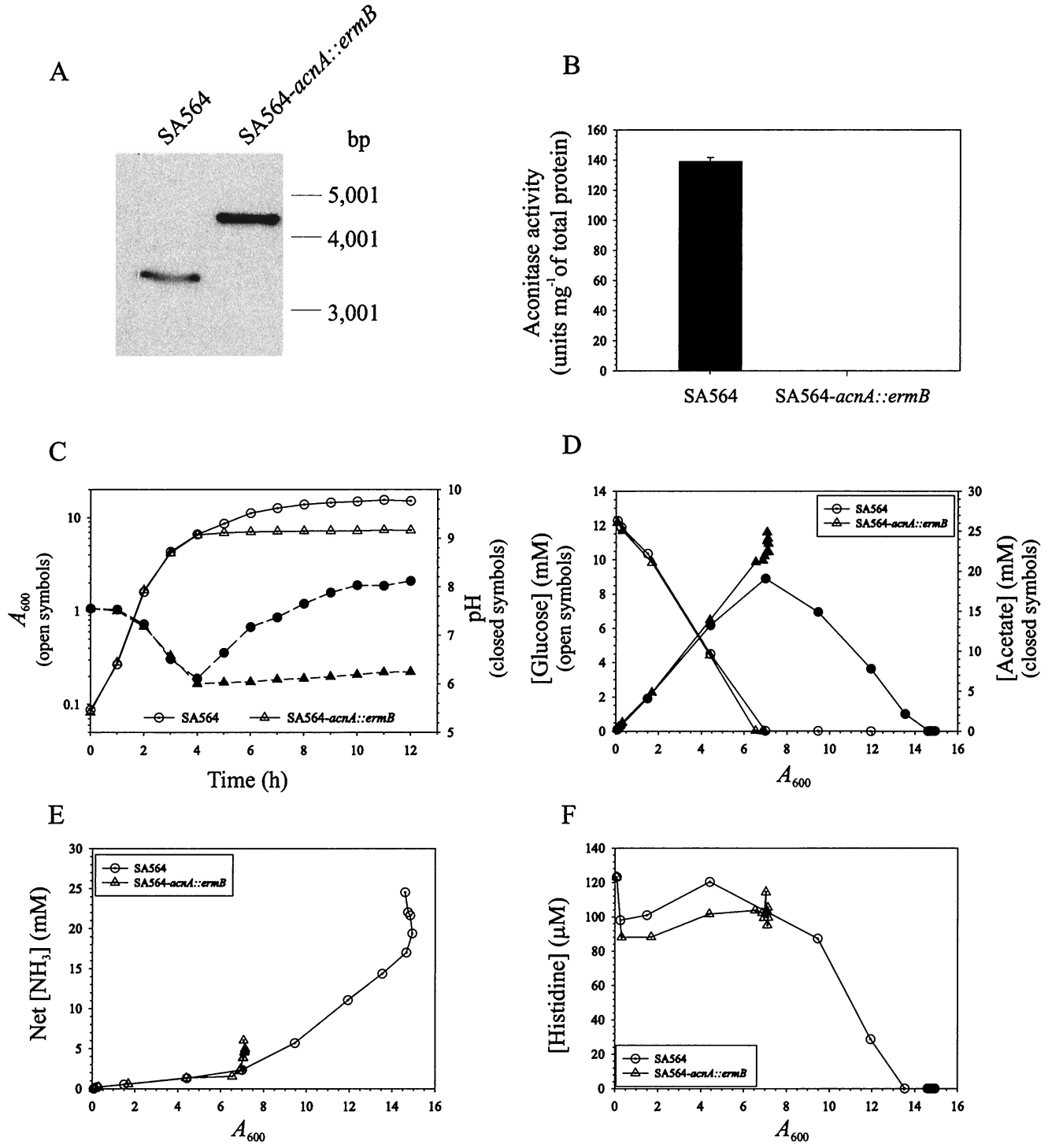

FIG. 1. Characteristics of the *S. aureus* aconitase mutant. (A) Southern blot confirmation of *acnA* disruption. Genomic DNA was isolated from strains SA564 and SA564-*acnA*::*ermB*, digested with *Eco*RI and *Eco*RV (the *acnA*-containing fragment is ~3,400 bp), and analyzed by Southern blotting. The *ermB* cassette was 1,280 bp, resulting in the ~4.6-kb band observed in the mutant strain. (B) Aconitase activities of strains SA564 and SA564-*acnA*::*ermB* after 6 h of growth. (C) The wild-type strain SA564 and the aconitase mutant strain SA564-*acnA*::*ermB* were grown in TSB. At the indicated times, an aliquot was removed, appropriate dilutions were made, and the absorbance at 600 nm was measured. (D) Glucose depletion and acetate accumulation and depletion in the culture supernatants of strain SA564 and strain SA564-*acnA*::*ermB* plotted as a function of growth. (E) Net ammonia accumulation in the culture supernatants of strains SA564 and SA564-*acnA*::*ermB*. (F) An example of postexponential free amino acid depletion from the culture medium. The results presented are representative of at least two independent experiments.

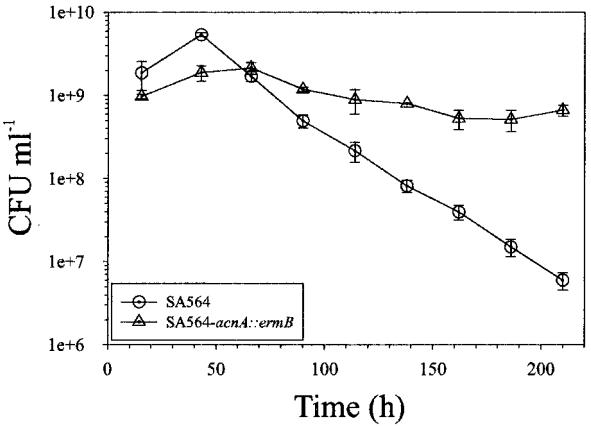

FIG. 2. TCA cycle inactivation enhances stationary-phase survival. Single colonies of SA564 and SA564-*acnA*::*ermB* were inoculated into TSB, grown at 37°C, and aerated by being shaken at 225 rpm for up to 2 weeks. At 24-h intervals, aliquots were removed and CFU per milliliter were determined in quadruplicate. The data presented are averages and standard deviations.

related organism *Bacillus subtilis* fails to sporulate during prolonged incubation, leading to the loss of viability (11). In contrast, the *S. aureus* aconitase mutant had greatly enhanced stationary-phase survival relative to the wild-type strain (Fig. 2). These data demonstrate that TCA cycle inactivation does not result in a premature death phase and indicate that a fully functioning TCA cycle is essential for normal cell lysis.

***S. aureus* aconitase mutant morphology.** Aconitase inactivation results in morphological defects in *B. subtilis* (11), *Streptomyces viridochromogenes* (36), and *Streptomyces coelicolor* (43). For example, a *B. subtilis* aconitase mutant failed to form a spore or an asymmetric septum (11), and *S. viridochromogenes* fails to form a normal aerial mycelium (36). To determine if aconitase inactivation affected *S. aureus* cell morphology, bacteria from exponentially growing (3-h) and stationary-phase (27-h) cultures of SA564 and SA564-*acnA*::*ermB* were examined by scanning electron microscopy (Fig. 3A to D). The gross morphologies of the aconitase mutant and wild-type strains were similar at both time points. However, the mutant and wild-type strains differed significantly in the maximal bacterial lengths (i.e., the longest distance across the bacterium). As expected, there was a significant decrease in the maximal length of wild-type strain SA564 cells during the transition from an exponentially growing culture to a stationary-phase culture (0.873 ± 0.049 and 0.719 ± 0.042 μm, respectively; $P > 0.0001$). However, there was no significant decrease in the maximal length of the aconitase mutant strain upon the transition from an exponentially growing culture to a stationary-phase culture (0.806 ± 0.079 and 0.745 ± 0.062 μm, respectively; $P = 0.09$). These data suggest that the premature entry into the stationary phase observed in the aconitase mutant incompletely blocks the size reduction of *S. aureus* that occurs during normal transition into the stationary phase of growth.

The significant difference in the maximal bacterial lengths could be the result of an alteration in cell wall thickness. To address this possibility, we examined strains SA564 and SA564-*acnA*::*ermB* using transmission electron microscopy during the exponential (3-h) and stationary (27-h) phases of growth (Fig. 3E to H). No alterations in the gross morphology or the cell wall thickness were observed in either the exponential or stationary phase of growth.

Glucose and acetate catabolism. *S. aureus* preferentially degrades glucose during growth (9, 18, 22, 28) (Fig. 1D). The primary pathways for the catabolism of glucose in *S. aureus* are the pentose phosphate and glycolytic pathways (4). The processing of glucose by the pentose phosphate pathway produces intermediates for purine biosynthesis and the glycolytic pathway intermediates fructose 6-phosphate and glyceraldehyde 3-phosphate; the last two compounds are then converted into pyruvate by glycolysis. The catabolic fate of pyruvate is determined by the growth conditions. During aerobic growth, pyruvate is enzymatically oxidized to acetyl-CoA and CO_2 by the pyruvate dehydrogenase complex (16). Additionally, acetyl-CoA can be further oxidized by the TCA cycle when grown in the presence of certain TCA cycle intermediates (18). To determine if inactivation of TCA cycle function altered the ability of *S. aureus* to catabolize glucose and/or acetate, we determined the concentrations of glucose and acetate in the culture supernatants of the wild-type and aconitase mutant strains grown in the presence of 0.25% glucose. Glucose was rapidly depleted from the culture media by both strains SA564 and SA564-*acnA*::*ermB* (Fig. 1D). Additionally, both strains accumulated acetate and acidified the culture media at equivalent rates during the exponential phase of growth (Fig. 1C and D). In contrast to a previous report (18), our data demonstrate that wild-type *S. aureus* begins to catabolize acetate at the end of the exponential phase of growth, and catabolism continues at a nearly constant rate until the acetate is depleted. However, the aconitase mutant strain does not catabolize acetate (Fig. 1D), demonstrating that a fully functioning TCA cycle is essential for acetate catabolism.

Inactivation of aconitase prevented the depletion of acetate from the culture medium, confirming that a metabolic block existed in the TCA cycle. A metabolic block can result in the accumulation of citrate in the medium and interfere with normal cellular processes (11). To examine this possibility, we measured the concentration of citric acid in the culture supernatant. Neither SA564 nor SA564-*acnA*::*ermB* accumulated citrate in the medium (data not shown). Additionally, the wild-type strain used citrate as a carbon source but the mutant did not, consistent with aconitase inactivation (data not shown). These data indicate that SA564-*acnA*::*ermB* does not generate excess citrate.

Amino acid catabolism. Catabolism of amino acids is usually accompanied by ammonia production. To measure amino acid degradation, the concentration of ammonia in the bacterial culture supernatants and the depletion of free amino acids were determined. The presence of glucose in the culture media incompletely suppressed ammonia generation in both SA564 and SA564-*acnA*::*ermB*, indicating an adequate supply of carbon for growth (Fig. 1E). However, upon depletion of the glucose, strain SA564 began to accumulate ammonia in the culture supernatant and to deplete free amino acids (Arg, Leu, Pro, and His [data not shown and Fig. 1F]), indicating that the culture medium had become carbon limited (Fig. 1E). In contrast, strain SA564-*acnA*::*ermB* failed to accumulate ammonia in the culture medium during the postexponential phase of growth, nor did it deplete free amino acids from the culture

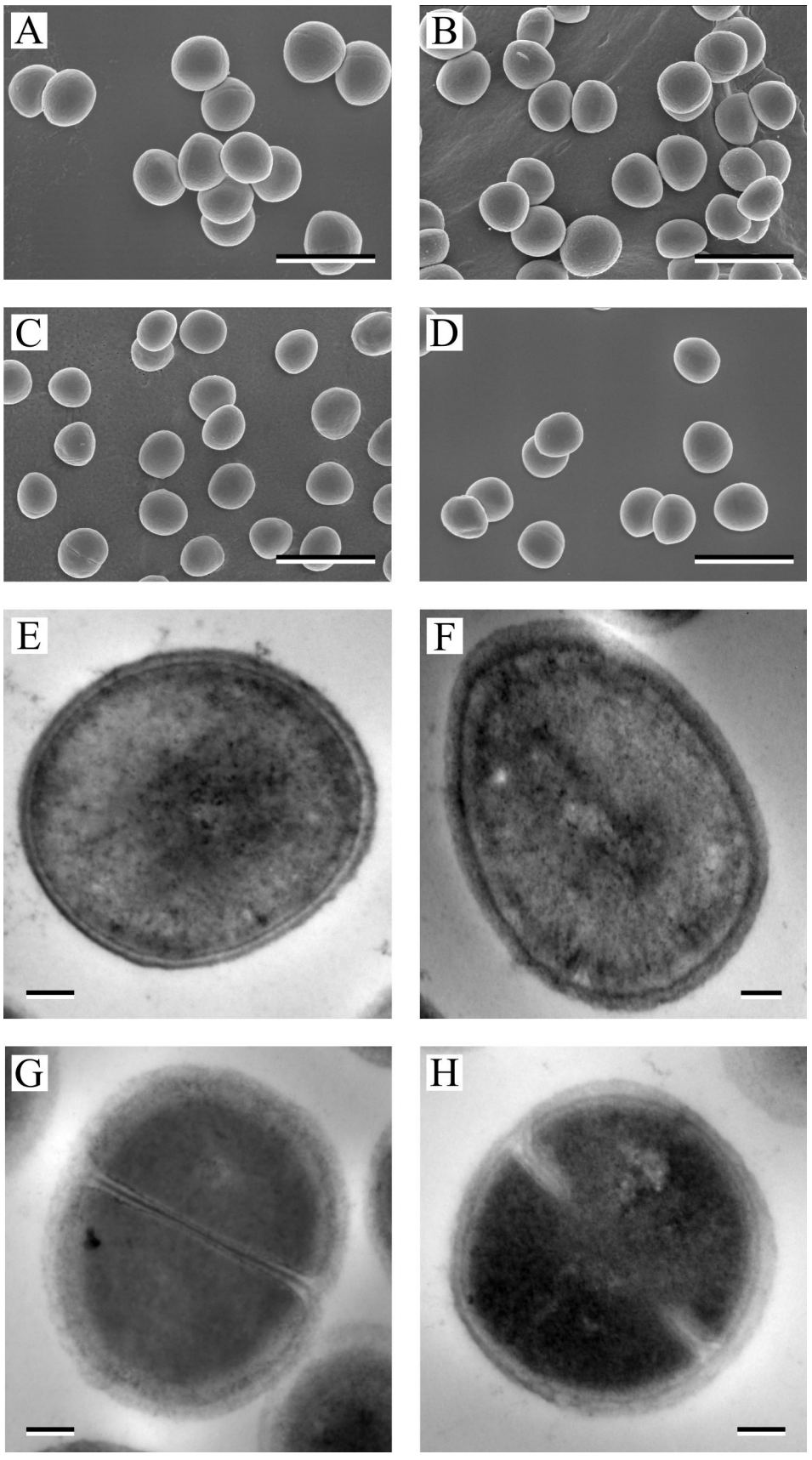

FIG. 3. Electron micrographs of SA564 and SA564-*acnA*::*ermB*. Scanning electron micrographs (A to D) of wild-type strain SA564 (A and C) or the aconitase mutant strain SA564-*acnA*::*ermB* (B and D) grown for either 3 (A and B) or 27 (C and D) h are shown. Transmission electron micrographs (E to H) of strain SA564 (E and G) or strain SA564-*acnA*::*ermB* (F and H) grown for either 3 (E and F) or 27 (G and H) h are shown. Bars, 1.5 μm (A to D) and 100 nm (E to H).

medium (Fig. 1E and F). These data indicate that a fully functioning TCA cycle is essential for amino acid catabolism.

Proteomic analysis of *S. aureus* culture supernatants. To test the effect of TCA cycle function on virulence factor production, we examined the production of extracellular proteins with 2-D electrophoresis of culture supernatants. Thirteen protein spots were selected for identification by peptide mass fingerprinting (Fig. 4). Protein spots 1 to 5 and 9 to 13 were chosen because they were absent or greatly reduced in supernatants prepared from strain SA564-*acnA*::*ermB* compared to those prepared from strain SA564. Protein spots 6, 7, and 8 were characterized because the intensities were predominantly invariant between the wild-type and mutant strains in repeated gels. All 13 protein spots were identified by MALDI-TOF MS analysis.

Protein spots 1, 2, and 3 are glycerol ester hydrolase (*geh*) (EC 3.1.1.3). The relative migration of the proteins isolated from the culture supernatants of the wild-type strain suggests that these three protein spots are degradation products of mature-form variants of lipase. There was a 50% reduction in total lipase activity in the culture supernatants of the mutant relative to those of the wild-type parental strain (data not shown). The presence of residual lipase activity is consistent with the production of a second lipase (see below). Protein spots 4 and 12 are a type C enterotoxin (SEC). The densities of spots 4 and 12 were twofold lower in the aconitase mutant relative to the wild-type strain. Enzyme-linked immunosorbent assays confirmed that the relative quantity of SEC present in the culture supernatant of the wild type (0.05 A_{405}/pg) was greater than in the aconitase mutant strain (0.02 A_{405}/pg). Protein spots 5, 9, and 13 are α-toxin (*hla*). Analysis of the hemolytic titers of culture supernatants confirmed that SA564-*acnA*::*ermB* had twofold less α-toxin activity than wild-type SA564 (data not shown). Protein spots 10 and 11 are serine protease variants. The culture supernatants were assayed for total protease activity, and no significant difference was detected.

Protein spot 6 is phospholipase C (EC 3.1.4.10). Protein spots 7 and 8 were tentatively identified as variant forms of lipase (EC 3.1.1.3). Based on genomic DNA sequence data available for *S. aureus* strain COL (http://www.tigr.org/), there are at least three genes that encode proteins with lipase activity. Taken together, these data indicate that TCA cycle inactivation had a pleiotropic effect on virulence factor production.

Characterization of production of additional virulence factors. *S. aureus* secretes or has on its cell surface several virulence factors that were not identified by 2-D gel analysis of the culture supernatants. To assess the effect of aconitase inactivation on the production of virulence factors not identified by proteomic analysis, we examined the bacteria for the presence of the fibrinogen receptor (clumping factor) and staphylokinase activity and examined culture supernatants for β-toxin activity and total protease activity. The wild-type SA564 strain clumped in the presence of fibrinogen, but the aconitase mutant did not. The levels of staphylokinase and protease activity were equivalent in the *acnA* mutant and the wild-type strain (data not shown). β-Toxin activity (encoded by *hlb*) in the culture supernatant of SA564-*acnA*::*ermB* was four times lower than in the wild-type strain (data not shown). Taken together, these data demonstrate that TCA cycle inactivation detrimentally affects the production of secreted virulence factors and cell-associated adhesion factors.

Analysis of RNAIII, *sarA*, and *sigB* RNA expression. The synthesis of many *S. aureus* virulence factors is regulated through an unknown mechanism by RNAIII, part of the *agr* operon. SarA indirectly regulates the expression of virulence factors by positively affecting the expression of RNAIII (8, 31). However, SarA can also act independently of *agr* to influence expression of virulence factors, such as α-toxin (7). The expression of *sarA* is in part regulated by σ^B (12). To examine the effect of TCA cycle inactivation on the level of RNAIII made by the wild-type and the aconitase mutant strains, we performed Northern blot analysis on total RNA isolated after 3 h (exponential phase) and 12 h (stationary phase) of growth. Significantly more RNAIII (14-fold higher) was present in the aconitase mutant than in the wild-type strain in the stationary phase (Fig. 5). However, the quantities of RNAIII detected in the mutant and wild-type strains were not significantly different in the exponential phase, consistent with our observation that TCA cycle inactivation does not alter exponential-phase growth.

The level of RNAIII has been shown to correlate with the level of SarA production (8), suggesting that increased transcription of *sarA* in the aconitase mutant was responsible for the enhanced expression of RNAIII. To test this hypothesis, Northern blot analysis of total RNA was done with a *sarA*-specific probe. The mutant strain had significantly (10-fold) more *sarA* mRNA than the wild-type strain in the exponential and stationary phases (Fig. 5). The stationary-phase increase in *sarA* mRNA coincided with an increase in RNAIII, consistent with the possibility that increased RNAIII is due to an increase in SarA. Interestingly, the expression of *sarA* was elevated in the aconitase mutant during exponential-phase growth, suggesting that TCA cycle function, or aconitase specifically, affects *sarA* regulation.

Inactivation of the gene (*sigB*) encoding σ^B increases expression of *sarA* (7). Therefore, the increased level of *sarA* mRNA detected in the aconitase mutant could be caused by decreased expression of *sigB*. However, expression of *sigB* in the *acnA* mutant in the exponential phase of growth was not substantially changed (Fig. 5). In contrast, *sigB* expression was dramatically lower in the stationary phase.

In the context of a current model of virulence gene regulation in *S. aureus* (33), the most likely explanation for these data is that inactivation of the TCA cycle prevents the post-exponential-phase continuance of *sigB* expression, yielding increased *sarA* expression and causing an increase in the expression of RNAIII. However, this model is incomplete, as it does not explain the increased *sarA* expression during the exponential phase of growth.

Virulence in a mouse soft-tissue infection model. Preliminary experiments indicated that aconitase inactivation did not significantly alter the ability of the mutant to cause disease in mice after intraperitoneal inoculation (data not shown). Therefore, to assess differences in gross pathology, we used a mouse soft-tissue infection model to measure the effect of aconitase inactivation on virulence. Mice infected with the aconitase mutant strain lost significantly more body weight than mice infected with the wild type (10.5% ± 3.5% versus 8.7% ± 3.1%; $P = 0.026$). Similarly, mice infected with the

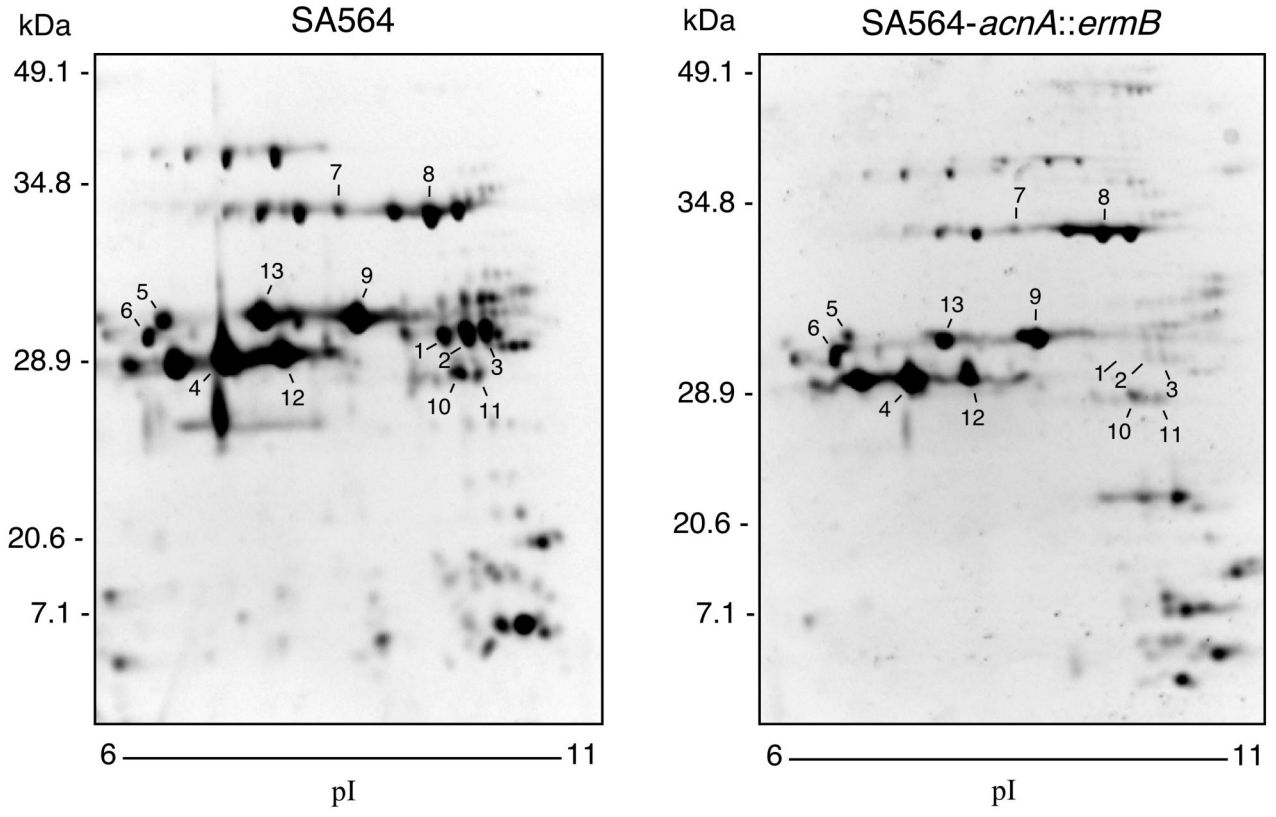

Protein spot(s)	Protein
1, 2, & 3	Glycerol ester hydrolase (Lipase)
4 & 12	Staphylococcal enterotoxin C (SEC)
5, 9, & 13	α-Toxin
6	Phospholipase C
7 & 8	Variant forms of lipase
10 & 11	Serine protease

FIG. 4. 2-D electrophoresis of SA564 and SA564-*acnA*::*ermB* culture supernatant proteins. Stationary-phase (12-h) culture supernatants were isolated from bacteria grown in protein-free TSB. Isoelectric focusing conducted with a pH 3 to 10 linear separation range showed that the majority of exoproteins had isoelectric points in the pH 6 to 10 range (data not shown). Therefore, subsequent isoelectric focusing was done with a linear separation range from pH 6 to 11. Protein spots analyzed by MALDI-TOF MS are indicated. The results are representative of multiple experiments using supernatant proteins from two independent isolations.

mutant organism required 5.8 ± 2.0 days to regain their pre-inoculation body weight, whereas animals inoculated with the wild-type strain required an average of 4 ± 1.2 days (P = 0.0005). Animals inoculated with the wild-type strain developed a marked ulceration at the injection site by the second day after infection, whereas animals infected with the mutant strain did not develop the same degree of ulceration until 4 or more days after inoculation (Fig. 6). Additionally, mice in-

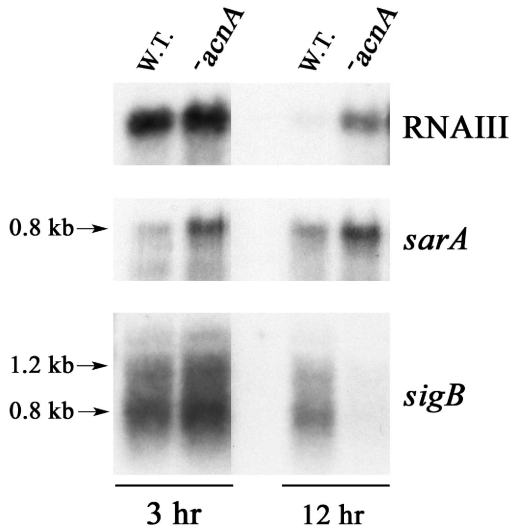

FIG. 5. Northern blot analysis of RNAIII, *sarA*, and *sigB* transcription. Total RNA was isolated from bacteria grown to exponential (3-h) and stationary (12-h) phases; 10 μg of total RNA was used per lane. To ensure that equivalent quantities of RNA were loaded, the RNA was visualized by ethidium bromide staining prior to transfer to a charged nylon membrane (data not shown). Radiolabeled probes specific for RNAIII, *sarA*, and *sigB* were used. The results presented are representative of multiple Northern blots with independently isolated total-RNA samples. W.T., wild type; ⁻acnA, SA564-*acnA*::*ermB*.

fected with the aconitase mutant took longer to reepithelize the ulcer site (Fig. 6). Although these data clearly indicate that aconitase inactivation altered pathogen-host interactions, the overall characters of the gross lesions in mice infected with the wild-type strain and the mutant strain were similar. The most notable difference in soft-tissue pathology between mice infected with the mutant and the wild-type strains was that the mutant-infected mice required a longer time to develop ulcers.

DISCUSSION

The existence of a TCA cycle in *S. aureus* was first reported in 1937 (24). However, an *S. aureus* allelic-replacement mutant in the TCA cycle had not been made prior to this study. In spite of this, some aspects of TCA cycle function were correctly deduced: acetate catabolism is mediated by the TCA cycle (18, 24, 39), and glucose represses TCA cycle activity (9, 18, 40). However, our study revealed many unexpected findings caused by TCA cycle inactivation: (i) TCA cycle inactivation completely prevents post-exponential-phase growth in a rich medium, (ii) a fully functional TCA cycle is necessary for maximal virulence factor production, (iii) TCA cycle inactivation alters pathogen-host interaction, and (iv) the TCA cycle is essential for entry into the death phase. These findings demonstrate the extent to which the TCA cycle is integrated into the life cycle of this critical human pathogen.

TCA cycle function during growth. *S. aureus* preferentially utilizes glucose via glycolysis during exponential-phase growth. The growth of bacteria with a functional TCA cycle under aerobic conditions can result in the incorporation of acetyl-CoA into citrate. This reaction is catalyzed by citrate synthase, the first enzyme of the TCA cycle. In *S. aureus*, the activity of citrate synthase does not increase until the bacteria enter the post-exponential phase (G. A. Somerville, unpublished data). Similarly, the levels of aconitase and isocitrate dehydrogenase activities, the second and third enzymes of the cycle, also increase upon entry into the post-exponential phase (Somerville, unpublished). Hence, carbon is not entering the TCA cycle during exponential-phase growth, and therefore, disruption of the TCA cycle would not be expected to alter exponential-phase growth. The observation that the wild type and the aconitase mutant have equivalent growth rates confirmed this hypothesis (Fig. 1C). However, upon depletion of glucose, TCA cycle function becomes essential for acetate catabolism

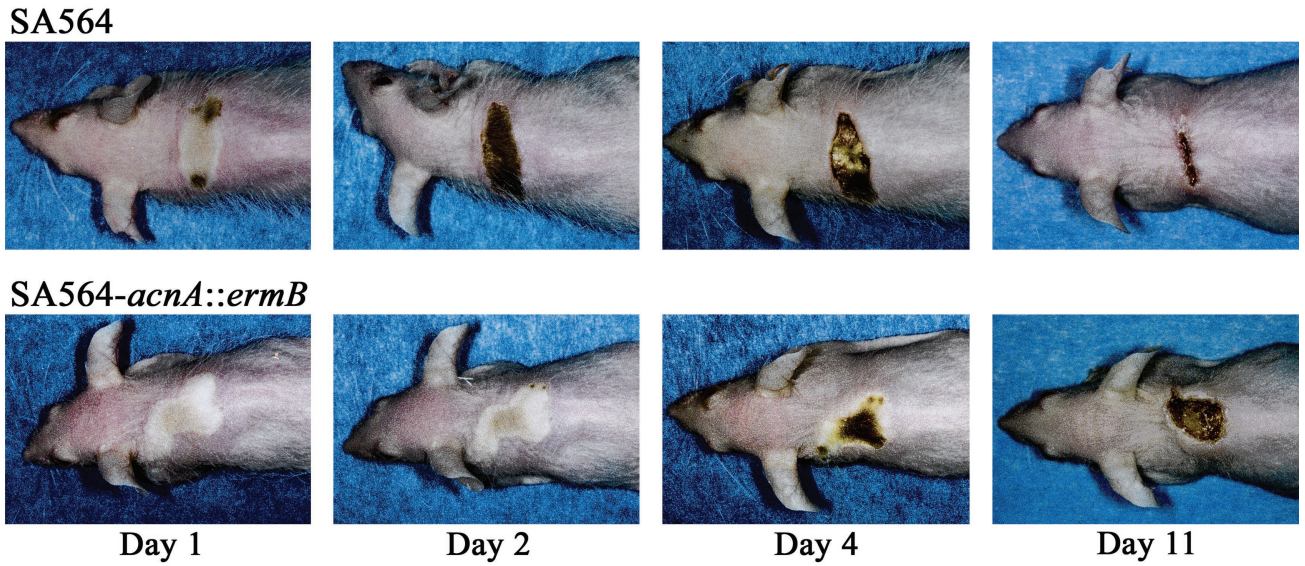

FIG. 6. Disease progression in mice infected subcutaneously with SA564 or SA564-*acnA*::*ermB*. Ten outbred, immunocompetent, hairless mice (Crl::SKH1-hrBR) were inoculated subcutaneously with 3×10^7 CFU of SA564 or SA564-*acnA*::*ermB*. Disease progression was followed for 18 days, and representative results are shown.

and post-exponential-phase growth (Fig. 1C and D). Surprisingly, TCA cycle inactivation also prevented the post-exponential growth phase catabolism of certain amino acids (Fig. 1F). If *S. aureus* withdraws TCA cycle intermediates for amino acid biosynthesis, then the available oxaloacetate is quickly depleted, thus precluding the introduction of acetyl-CoA into the cycle. Therefore, for *S. aureus* to gain energy from the TCA cycle by acetate catabolism, it must have a pool of TCA cycle intermediates to provide C_4 or C_5 intermediates. These intermediates can be supplied by the catabolism of amino acids, an idea put forth previously (18). Taken together, these data demonstrate that acetate and amino acid catabolism is essential for post-exponential-phase growth under aerobic growth conditions.

TCA cycle function and virulence factor production. In the absence of a functional TCA cycle, the production of several virulence factors was significantly reduced (Fig. 4). The simplest explanation for the decreased production of virulence factors is that the premature entry into the stationary phase circumvents the normal post-exponential growth phase production of virulence factors. Implicit in this hypothesis is that the production of all virulence factors should be affected equally; however, this was not the case. We found that the production of α- and β-toxins, glycerol ester hydrolase (lipase), and SEC was decreased in the isogenic mutant (Fig. 4 and data not shown), but production of staphylokinase, total protease, and variant forms of lipase was unchanged. An additional explanation is that an alteration in the expression of the global gene regulator RNAIII, *sarA*, or *sigB* (Fig. 5) causes pleiotropic effects on virulence factor synthesis. However, the exact role of the TCA cycle in virulence factor production remains to be elucidated.

Aconitase inactivation, virulence, and in vivo mutagenesis screening. TCA cycle inactivation dramatically altered the life cycle of *S. aureus*. Thus, it is surprising that three independent in vivo mutagenesis screens failed to uniformly identify TCA cycle enzymes as important in virulence (10, 25, 30). However, a possible explanation is that each of the three studies used the highly passaged *S. aureus* strain RN6390. Recently, we demonstrated that *S. aureus* undergoes significant phenotypic and genotypic changes during serial passage (37). Specifically, we demonstrated that passage of *S. aureus* decreases TCA cycle function by decreasing aconitase activity. Additionally, all mutagenesis screens were conducted with mice, which are not normally infected by *S. aureus*; thus, detecting subtle changes in host-pathogen interactions requires greater vigilance or a different animal model. Consistent with this, our mouse soft-tissue infection results indicate that disruption of aconitase significantly alters pathogen-host interaction but does not substantially decrease virulence in this animal model. The altered pathogen-host interaction is most likely due to decreased virulence factor production, decreased growth yield, or enhanced stationary-phase survival.

Implications for TCA cycle inactivation in vivo. Phagocytic leukocytes use reactive oxygen species (superoxide radicals, hydrogen peroxide, and hydroxyl radicals) to control microbial pathogens as an important part of the innate immune response (2). The enzymatic activity of aconitase is mediated by an essential iron-sulfur center [4Fe-4S] that is especially susceptible to inactivation by oxygen radicals (17). Oxidative loss of the fourth Fe atom produces an enzyme that is in the [3Fe-4S] state, resulting in reversible inactivation of aconitase and the TCA cycle. Our data demonstrated that genetically inactivating the TCA cycle induced an unusual and unexpected phenotype characterized by premature entry into the stationary phase (Fig. 1C) and enhanced survival (Fig. 2). Hence, we speculate that reversible aconitase inactivation in wild-type *S. aureus* is a survival response to oxidative stress induced during host-pathogen interactions. This hypothesis might also explain the delayed disease resolution in mice infected with the aconitase mutant strain (Fig. 6) (i.e., the mutant bacteria are better able to survive, and thus, bacterial clearance is delayed). Although speculative, it is possible that aconitase inactivation contributes to prolonged survival within a host.

Possible role for aconitase in addition to its enzymatic function. Aconitase is a TCA cycle enzyme that converts citrate to isocitrate via a *cis*-aconitate intermediate. Eukaryotic organisms have mitochondrial and cytoplasmic aconitase activities (20). The cytoplasmic aconitase activity is caused by the iron-responsive protein-1 (IRP-1), an mRNA-binding protein that posttranscriptionally regulates the synthesis of iron-regulated proteins (21). Thus, cytosolic aconitase is a bifunctional protein. Recently, it has been demonstrated that aconitases from *B. subtilis* and *E. coli* bind to elements in mRNAs in an iron-dependent fashion (1, 41, 42). These observations established bacterial aconitase, like eukaryotic cytosolic aconitase (IRP-1), as a bifunctional protein. Determining if aconitase has a regulatory role in *S. aureus* virulence factor production is under way.

ACKNOWLEDGMENTS

We thank R. Cole for technical assistance; G. Hettrick and A. Mora for help with figure preparation; M. Parnell, J. Bailey, R. Larson, and B. Charles of the Veterinary Branch for help with the animal experiments; and M. Otto and F. Gherardini for critical review of the manuscript.

REFERENCES

1. **Alen, C., and A. L. Sonenshein.** 1999. *Bacillus subtilis* aconitase is an RNA-binding protein. Proc. Natl. Acad. Sci. USA **96:**10412–10417.
2. **Babior, B. M.** 2000. Phagocytes and oxidative stress. Am. J. Med. **109:**33–44.
3. **Baughn, A. D., and M. H. Malamy.** 2002. A mitochondrial-like aconitase in the bacterium *Bacteroides fragilis*: implications for the evolution of the mitochondrial Krebs cycle. Proc. Natl. Acad. Sci. USA **99:**4662–4667.
4. **Blumenthal, H. J.** 1972. Glucose catabolism in staphylococci, p. 111–135. *In* J. O. Cohen (ed.), The staphylococci. Wiley-Interscience, New York, N.Y.
5. **Bruckner, R.** 1997. Gene replacement in *Staphylococcus carnosus* and *Staphylococcus xylosus*. FEMS Microbiol. Lett. **151:**1–8.
6. **Chaussee, M. S., R. O. Watson, J. C. Smoot, and J. M. Musser.** 2001. Identification of Rgg-regulated exoproteins of *Streptococcus pyogenes*. Infect. Immun. **69:**822–831.
7. **Cheung, A. L., Y. T. Chien, and A. S. Bayer.** 1999. Hyperproduction of alpha-hemolysin in a *sigB* mutant is associated with elevated SarA expression in *Staphylococcus aureus*. Infect. Immun. **67:**1331–1337.
8. **Chien, Y., A. C. Manna, and A. L. Cheung.** 1998. SarA level is a determinant of *agr* activation in *Staphylococcus aureus*. Mol. Microbiol. **30:**991–1001.
9. **Collins, F. M., and J. Lascelles.** 1962. The effect of growth conditions on oxidative and dehydrogenase activity in *Staphylococcus aureus*. J. Gen. Microbiol. **29:**531–535.
10. **Coulter, S. N., W. R. Schwan, E. Y. Ng, M. H. Langhorne, H. D. Ritchie, S. Westbrock-Wadman, W. O. Hufnagle, K. R. Folger, A. S. Bayer, and C. K. Stover.** 1998. *Staphylococcus aureus* genetic loci impacting growth and survival in multiple infection environments. Mol. Microbiol. **30:**393–404.
11. **Craig, J. E., M. J. Ford, D. C. Blaydon, and A. L. Sonenshein.** 1997. A null mutation in the *Bacillus subtilis* aconitase gene causes a block in Spo0A-phosphate-dependent gene expression. J. Bacteriol. **179:**7351–7359.
12. **Deora, R., T. Tseng, and T. K. Misra.** 1997. Alternative transcription factor sigma B of *Staphylococcus aureus*: characterization and role in transcription of the global regulatory locus *sar*. J. Bacteriol. **179:**6355–6359.

13. **Dorward, D. W.** 1999. Interactions between mouse lymphocytes and *Borrelia burgdorferi*, the infectious agent of Lyme disease, p. 1242–1243. *In* G. W. Bailey (ed.), Microscopy and microanalysis, vol. 5. Springer-Verlag, New York, N.Y.
14. **Fitzgerald, J. R., P. J. Hartigan, W. J. Meaney, and C. J. Smyth.** 2000. Molecular population and virulence factor analysis of *Staphylococcus aureus* from bovine intramammary infection. J. Appl. Microbiol. **88:**1028–1037.
15. **Foster, T. J.** 1998. Molecular genetic analysis of staphylococcal virulence, p. 433–454. *In* P. Williams, J. Ketley, and G. P. C. Salmond (ed.), Methods in microbiology, bacterial pathogenesis, vol. 27. Academic Press, Inc., San Diego, Calif.
16. **Gardner, J. F., and J. Lascelles.** 1962. The requirement for acetate of a streptomycin-resistant strain of *Staphylococcus aureus*. J. Gen. Microbiol. **29:**157–164.
17. **Gardner, P. R., and I. Fridovich.** 1992. Inactivation-reactivation of aconitase in *Escherichia coli*. A sensitive measure of superoxide radical. J. Biol. Chem. **267:**8757–8763.
18. **Goldschmidt, M. C., and D. M. Powelson.** 1953. Effect of the culture medium on the oxidation of acetate by *Micrococcus pyogenes* var. aureus. Arch. Biochem. Biophys. **46:**154–163.
19. **Greene, C., D. McDevitt, P. Francois, P. E. Vaudaux, D. P. Lew, and T. J. Foster.** 1995. Adhesion properties of mutants of *Staphylococcus aureus* defective in fibronectin-binding proteins and studies on the expression of *fnb* genes. Mol. Microbiol. **17:**1143–1152.
20. **Henson, C. P., and W. W. Cleland.** 1967. Purification and kinetic studies of beef liver cytoplasmic aconitase. J. Biol. Chem. **242:**3833–3838.
21. **Kaptain, S., W. E. Downey, C. Tang, C. Philpott, D. Haile, D. G. Orloff, J. B. Harford, T. A. Rouault, and R. D. Klausner.** 1991. A regulated RNA binding protein also possesses aconitase activity. Proc. Natl. Acad. Sci. USA **88:** 10109–10113.
22. **Kendall, A. I., T. E. Friedemann, and M. Ishikawa.** 1930. Quantitative observations on the chemical activity of "resting" *Staphylococcus aureus.* J. Infect. Dis. **47:**223–228.
23. **Kennedy, M. C., M. H. Emptage, J. L. Dreyer, and H. Beinert.** 1983. The role of iron in the activation-inactivation of aconitase. J. Biol. Chem. **258:**11098–11105.
24. **Krebs, H. A.** 1937. Dismutation of pyruvic acid in *Gonococcus* and *Staphylococcus*. Biochem. J. **31:**661–671.
25. **Lowe, A. M., D. T. Beattie, and R. L. Deresiewicz.** 1998. Identification of novel staphylococcal virulence genes by in vivo expression technology. Mol. Microbiol. **27:**967–976.
26. **Lowry, O. H., N. J. Rosebrough, L. Farr, and R. J. Randall.** 1951. Protein measurement with the Folin phenol reagent. J. Biol. Chem. **193:**267–275.
27. **Lukomski, S., C. A. Montgomery, J. Rurangirwa, R. S. Geske, J. P. Barrish, G. J. Adams, and J. M. Musser.** 1999. Extracellular cysteine protease produced by *Streptococcus pyogenes* participates in the pathogenesis of invasive skin infection and dissemination in mice. Infect. Immun. **67:**1779–1788.
28. **Mah, R. A., D. Y. Fung, and S. A. Morse.** 1967. Nutritional requirements of *Staphylococcus aureus* S-6. Appl. Microbiol. **15:**866–870.
29. **McDonald, K.** 1984. Osmium ferricyanide fixation improves microfilament preservation and membrane visualization in a variety of animal cell types. J. Ultrastruct. Res. **86:**107–118.
30. **Mei, J. M., F. Nourbakhsh, C. W. Ford, and D. W. Holden.** 1997. Identification of *Staphylococcus aureus* virulence genes in a murine model of bacteraemia using signature-tagged mutagenesis. Mol. Microbiol. **26:**399–407.
31. **Morfeldt, E., K. Tegmark, and S. Arvidson.** 1996. Transcriptional control of the *agr*-dependent virulence gene regulator, RNAIII, in *Staphylococcus aureus*. Mol. Microbiol. **21:**1227–1237.
32. **Novick, R. P.** 1991. Genetic systems in staphylococci. Methods Enzymol. **204:**587–636.
33. **Novick, R. P.** 2000. Pathogenicity factors and their regulation, p. 392–407. *In* V. A. Fischetti, R. P. Novick, J. J. Ferretti, D. A. Portnoy, and J. I. Rood (ed.), Gram-positive pathogens. ASM Press, Washington, D.C.
34. **Sambrook, J., E. F. Fritsch, and T. Maniatis.** 1989. Molecular cloning: a laboratory manual, 2nd ed. Cold Spring Harbor Laboratory Press, Cold Spring Harbor, N.Y.
35. **Schenk, S., and R. A. Laddaga.** 1992. Improved method for electroporation of *Staphylococcus aureus*. FEMS Microbiol. Lett. **73:**133–138.
36. **Schwartz, D., S. Kaspar, G. Kienzlen, K. Muschko, and W. Wohlleben.** 1999. Inactivation of the tricarboxylic acid cycle aconitase gene from *Streptomyces viridochromogenes* Tu494 impairs morphological and physiological differentiation. J. Bacteriol. **181:**7131–7135.
37. **Somerville, G. A., S. B. Beres, J. R. Fitzgerald, F. R. DeLeo, R. L. Cole, J. S. Hoff, and J. M. Musser.** 2002. In vitro serial passage of *Staphylococcus aureus*: changes in physiology, virulence factor production, and *agr* nucleotide sequence. J. Bacteriol. **184:**1430–1437.
38. **Southern, E. M.** 1975. Detection of specific sequences among DNA fragments separated by gel electrophoresis. J. Mol. Biol. **98:**503–517.
39. **Stedman, R. L., and E. Kravitz.** 1955. Evidence for a common pathway for pyruvate and acetate oxidation by *Micrococcus pyogenes* var. aureus. Arch. Biochem. Biophys. **59:**260–268.
40. **Strasters, K. C., and K. C. Winkler.** 1963. Carbohydrate metabolism of *Staphylococcus aureus*. J. Gen. Microbiol. **33:**213–229.
41. **Tang, Y., and J. R. Guest.** 1999. Direct evidence for mRNA binding and post-transcriptional regulation by *Escherichia coli* aconitases. Microbiology **145:**3069–3079.
42. **Tang, Y., M. A. Quail, P. J. Artymiuk, J. R. Guest, and J. Green.** 2002. *Escherichia coli* aconitases and oxidative stress: post-transcriptional regulation of *sodA* expression. Microbiology **148:**1027–1037.
43. **Viollier, P. H., K. T. Nguyen, W. Minas, M. Folcher, G. E. Dale, and C. J. Thompson.** 2001. Roles of aconitase in growth, metabolism, and morphological differentiation of *Streptomyces coelicolor*. J. Bacteriol. **183:**3193–3203.

Editor: D. L. Burns